Blends of Polypropylene with Poly(*cis*-butadiene) Rubber. III. Study on the Phase Structure and Morphology of Incompatible Blends of Polypropylene with Poly(*cis*-butadiene) Rubber

Gui-Qiu Ma, Yun-Hui Zhao, Li-Tang Yan, Yun-Yan Li, Jing Sheng

School of Materials Science and Engineering, Tianjin University, Tianjin 300072, People's Republic of China

Received 17 February 2005; accepted 28 July 2005
DOI 10.1002/app.23499
Published online in Wiley InterScience (www.interscience.wiley.com).

ABSTRACT: Scanning electron microscopy (SEM) was used to study the structure and morphology of partly compatible binary blends of polypropylene with poly(*cis*-butadiene) rubber. The SEM images were transformed by digital image process software designed by our group, and binarized images were obtained. The size (mean diameters d_p and characteristic lengths L) of phases was calculated using binarized images. Small-angle light scattering was employed to study the structure and morphology of phases in the blends. The structural parameters, including correlation distance a_c, average chord lengths $\bar{l}$, and mean diameter D_S to describe the structure and morphology of phases in binary blends, were calculated based on the corresponding theory. The variation of correlation distance a_c, average chord length $\bar{l}$, and mean diameter D_S were the same as that of mean diameters d_p and characteristic length L. At the same time, the distribution of sizes of the dispersed phase in binary blends was calculated with graph transition technique, which possessed log-normal distribution characterization. The power spectrum images corresponding to small-angle light scattering images were obtained by two-dimensional fourier transformation of binary images. The correlation distances a_{cf} and average chord length $\bar{l}_f$ have been calculated by intensity of power spectrum images and that was the same as a_c and $\bar{l}$. © 2006 Wiley Periodicals, Inc. J Appl Polym Sci 100: 4900–4909, 2006

Key words: blends; isotactic poly(propylene); poly(*cis*-butadiene) rubber; light scattering; SEM

INTRODUCTION

In the our first preceding paper,[1] the phase structure and morphology of partly compatible binary blends of isotactic polypropylene (iPP) with ethyl acrylate grafting onto poly(*cis*-butadiene) rubber (PcBR-*g*-EA) were studied by small-angle X-ray scattering (SAXS), scanning electron microscope (SEM), and IR spectra. The compatibility of the blends of iPP with PcBR-*g*-EA was studied by SAXS. The part-compatibility of the blends was proven and the thickness of interface layer between the two phases in the blends was calculated. This suggests that a dilute dispersed PcBR-*g*-EA or iPP in the blends was molecularly distributed. The aggregates increase in size with an increase in the concentration of PcBR-*g*-EA or iPP.

In the second preceding paper,[2] the phase structure and morphology of incompatible binary blends of iPP/PcBR were studied by a method identical to that in the first paper. The incompatibility of iPP with PcBR was proven by SAXS, and an interface layer did not exist between the two phases in the blends of iPP/PcBR. But the dispersion of phases was even in the blends of iPP/PcBR. Similarly, a dilute dispersed PcBR or iPP in the iPP/PcBR blends was molecularly distributed, and the aggregates increase in size with an increase in concentration of PcBR or iPP.

A lot of used thermoplastic materials show marked limitation in their use when toughness and high impact resistance are required.[3] These limitations may be overcome by melt-mixing these materials with a rubber polymer. But if the two phases in the thermoplastic/rubber blends are incompatible, the thermoplastic can not be modified easily. Clearly, improvement of the compatibility of the two phases in heterogeneous polymer blends by adding a small amount of compatibilizer (grafted or block copolymers) is a topic of major practical significance. However, the study on the phase structure and morphology of incompatible blends is very important when the compatibility of heterogeneous polymer blends is being studied.

The phase structure and morphology can be studied by several means, including light microscope, electron microscope, light scattering (especially small-angle

Correspondence to: J. Sheng (shengxu@public.tpt.tj.cn).
Contract grant sponsor: National Natural Science Foundation of China; contract grant number: 50390090.

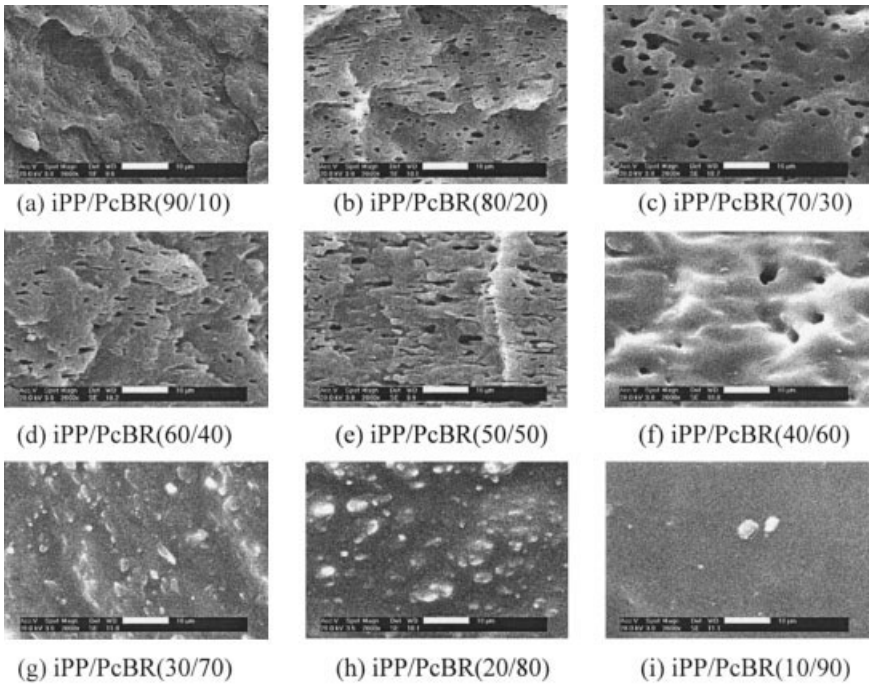

Figure 1 SEM images of iPP/PcBR blends (Bars correspond 10 μm).(a) iPP/PcBR (90/10), (b) iPP/PcBR (80/20), (c) iPP/PcBR (70/30), (d) iPP/PcBR (60/40), (e) iPP/PcBR (50/50), (f) iPP/PcBR (40/60), (g) iPP/PcBR(30/70), (h) iPP/PcBR (20/80), (i) iPP/PcBR (10/90).

light scattering (SALS) and SAXS), AFM, etc. In this article, we discuss the phase structure and morphology of iPP/PcBR blends using SALS and SEM. The structural parameters were calculated from the data of SALS in iPP/PcBR blends. Also, the morphology and graphical analysis of the phase structure in these blends were observed by SEM. At the same time, the binarized images were obtained by the digital image processing technique, and the power spectrum images were obtained using two-dimensional Fourier transformation (2DFT).[4]

EXPERIMENTAL

Materials

Isotactic Polypropylene (iPP) [melt index (MI) = 8, molecular weight = 5.0×10^5] and Poly(*cis*-butadiene) rubber (Mooney viscosity = 45), obtained from the Yanshan Petrochemical Co. (Beijing, China), were used.

Preparation of blends

Binary blends of iPP/PcBR were made by melt-mixing the polymer in a mixing apparatus (XXS-30 mixer, China) at a temperature of 210°C, with a residence time of 5 min, at 32 rpm.

The compositions of the binary blends of iPP/PcBR were 90/10, 80/20, 70/30, 60/40, 50/50, 40/60, 30/70, 20/80, and 10/90 (iPP wt %/PcBR wt %), i.e., 89.96/10.04, 79.93/20.07, 69.91/30.09, 59.89/40.11, 49.89/50.11, 39.89/60.11, 29.9/70.1, 19.92/80.08, and 9.96/90.04 (iPP vol %/PcBR vol %).

Specimen preparation

The premixed material was compression-molded to get slabs of 1-mm thickness and a film of less than 100 μm thickness at 230°C with a residence time of 5 min in a common heated press (24.5 MPa). The slabs of 1-mm thickness were broken in liquid nitrogen for observation under a SEM. The film of less than 100 μm thickness was used in the SALS tests.

RESULTS AND DISCUSSION

The overall morphology of the blends of iPP/PcBR has been investigated on the fractured surface of specimens broken in liquid nitrogen. The fractured surface of the samples is etched by cyclohexane. Hereby, the rubber phase is etched off with black holes left. SEM images of cryogenically fractured surface of the iPP/PcBR blends are shown in Figure 1. As can be seen, the phase-inversion region is from a composition of 50/50 to 30/70 wt % in the blends. Before 50/50 wt %, the PcBR is the dispersed phase, and it exhibits a hole-like morphology uniformly distributed throughout the whole sample. After 30/70 wt %, iPP becomes the

TABLE I
Ratio between Long Axis and Short Axis of Particles

iPP/PcBR compostion	l_{max}/l_{min}
10/90	1.1381
20/80	1.1639
40/60	1.3148
50/50	1.7708
70/30	1.2105
80/20	1.3235
90/10	1.0875

TABLE II
The Size of Phases in iPP/PcBR Blends by SEM

iPP (wt %)	Particle number	L_1 (μm)	L_2 (μm)	d_P (μm)
10	29	1.96	12.44	1.58
20	81	1.22	10.53	1.39
30	63	1.04	11.78	1.28
40	50	2.48	21.62	3.10
50	87	1.25	7.46	1.67
60	85	1.07	8.35	1.33
70	84	1.44	8.61	1.69
80	218	1.004	5.57	1.18
90	312	0.73	6.17	0.82

dispersed phase. In the phase-inversion region, a double continuous phase is formed in the blends of iPP/PcBR. For different compositions of iPP/PcBR with particle/matrix structure, the mean ratio between long axis and short axis of particles L_{max}/L_{min} is given in Table I. In view of the smaller value of L_{max}/L_{min}, it is effective to regard the dispersed particles as ellipses and study the structure of blends in terms of the corresponding light scattering theory, which will de discussed later.

The SEM images show structure and morphology of phases on the fractured surfaces in the blends. But if we calculate the size of phases using SEM images, it had better abstract such physical information as the particles of dispersed phases from SEM images. Therefore, the SEM images need to be transformed by digital image process software designed by our group. These results, i.e., the binarized images, are obtained and shown in Figure 2.

The size (average diameter d_p and characteristic lengths L_1 and L_1, whose significance is similar to that of l_1 and l_2, see Fig. 10) and distribution of sizes of the dispersed phase in the blends were calculated by the graph-analysis methods on binary images, and the result is shown in Table II and Figure 3.

Figure 4 shows the variation of d_p and characteristic length of dispersed phases $L_{d(SEM)}$ as function of weight fraction of iPP. It can be found that the values of diameter d_p are the similar to those of the characteristic lengths $L_{d(SEM)}$, and also, the values increase as the weight fraction of dispersed phases increase.

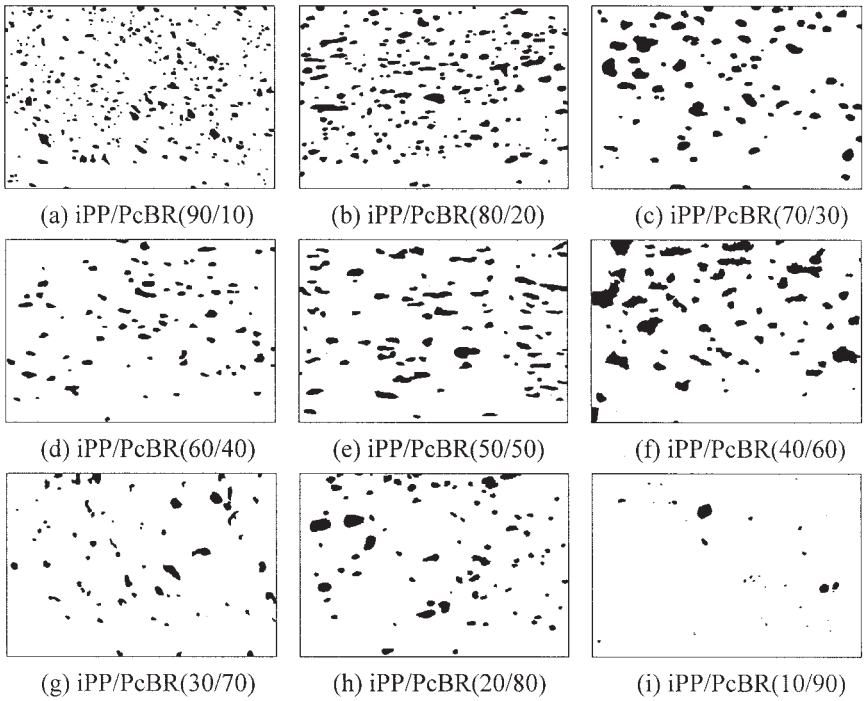

Figure 2 Binary images of iPP/PcBR blends. (a) iPP/PcBR (90/10), (b) iPP/PcBR (80/20), (c) iPP/PcBR (70/30), (d) iPP/PcBR (60/40), (e) iPP/PcBR (50/50), (f) iPP/PcBR (40/60), (g) iPP/PcBR (30/70), (h) iPP/PcBR (20/80), (i) iPP/PcBR (10/90).

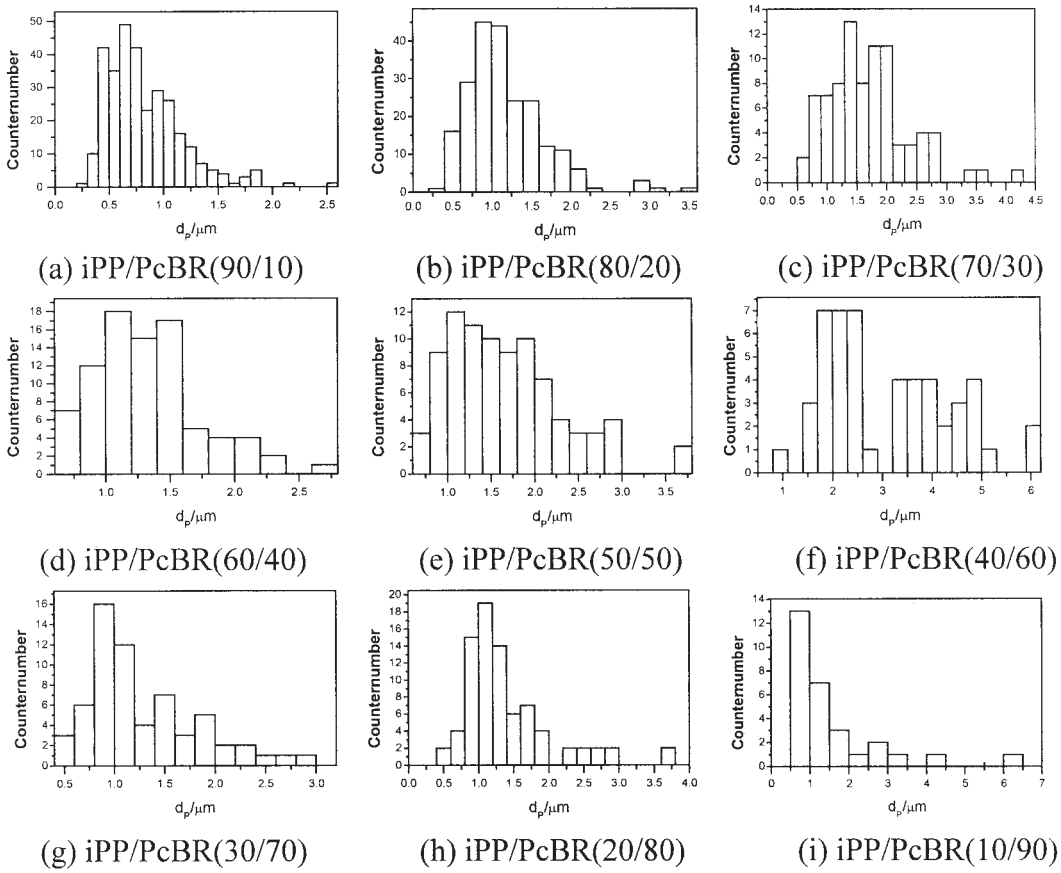

Figure 3 Histogram of d_p of iPP/PcBR blends. (a) iPP/PcBR (90/10), (b) iPP/PcBR (80/20), (c) iPP/PcBR (70/30), (d) iPP/PcBR (60/40), (e) iPP/PcBR (50/50), (f) iPP/PcBR (40/60), (g) iPP/PcBR (30/70), (h) iPP/PcBR (20/80), (i) iPP/PcBR(10/90).

To study the distribution of sizes quantitatively, a graphical method based on a log-normal distribution was employed.[5] If the probability distribution of a random positive variable x is normal (i.e., Gaussian), it is conventional to express this property as follows:

$$x \sim N(\mu,\sigma^2) \tag{1}$$

where μ is the mean, σ is the standard deviation, and σ^2 is the variance. For a log-normal distribution, the variable x is simply replaced with $\log(t)$. The cumulative probability is then

$$F(t) = \frac{1}{\sqrt{2\pi}} \int_{-\infty}^{\frac{\log t-\mu}{\sigma}} \exp\left[-\frac{x^2}{2}\right] dx = \Phi\left(\frac{\log t-\mu}{\sigma}\right) \quad \text{for } t > 0 \tag{2}$$

Since the cumulative probability function increases monotonically with x, an inverse function exists, and is given by

$$\Phi^{-1}[F(t)] = \frac{\log t-\mu}{\sigma} \tag{3}$$

writing $\Phi^{-1}[F(t)] = Y$, and $\log(t) = X$, eq. (3) can then be written as

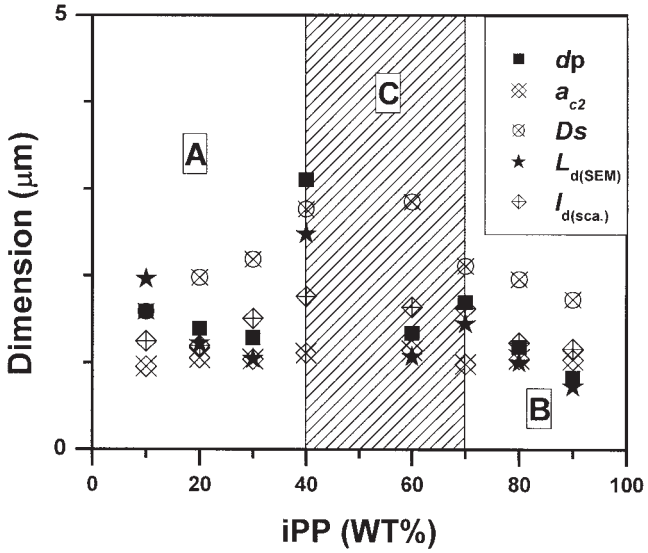

Figure 4 Relation of diameters d_p, $L_{d(SEM)}$, a_{c2}, D_s, and $l_{d(sca.)}$ of dispersed phases with compositions in iPP/PcBR blends.

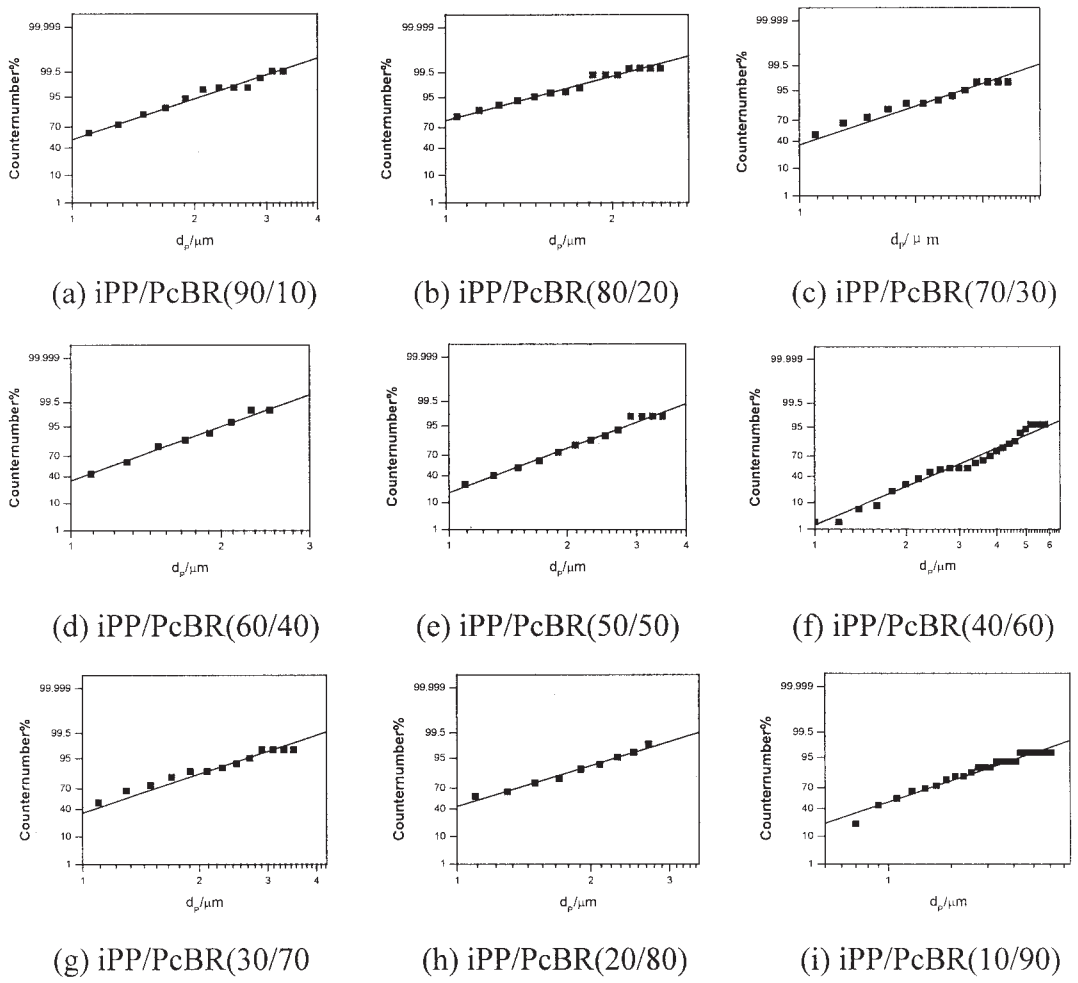

Figure 5 Cumulative distribution of particle diameters of dispersed phases. (a) iPP/PcBR (90/10), (b) iPP/PcBR (80/20), (c) iPP/PcBR (70/30), (d) iPP/PcBR (60/40), (e) iPP/PcBR (50/50), (f) iPP/PcBR (40/60), (g) iPP/PcBR (30/70), (h) iPP/PcBR (20/80), (i) iPP/PcBR (10/90).

$$Y = \frac{1}{\sigma} X - \frac{\mu}{\sigma} \tag{4}$$

Equation (4) corresponds to a straight line in the X–Y reference frame whose slope is $1/\sigma$ and intercept is $-\mu/\sigma$. Thus, the relation between a log-normal distribution function and an increasing straight line in the X-Y reference frame is found, which is described as the graph-estimation method. Based on the method, it can be judged whether the distribution of sizes of the dispersed phase is a log-normal distribution and the distribution width of sizes can be obtained.

Figure 5 is the cumulative distribution of particle diameters of dispersed phases in the blends of iPP/PcBR, which is obtained from Figure 3. Clearly, the cumulative distribution of particle diameters of dispersed phases possesses a linear relationship. Therefore, the distribution of dispersed phases in the blends of iPP/PcBR obeys the log-normal distribution, and the distribution of sizes can be studied in detail using the corresponding parameter σ of log-normal distribution. Figure 6 depicts the relation between σ and different compositions. When iPP concentration is increased, σ decreases and the distribution of particle diameters of dispersed phases in the blends of iPP/PcBR becomes more narrow.

Using 2DFT, the power spectrum image can be obtained, which is shown in Figure 7. We can see that the facula on the power spectrum image is basically round when the content of dispersed phases is smaller. When the content of dispersed phases is higher, especially at 50/50 wt %, the facula is elliptical, because of the distortion of particles. Besides, the direction of the longer axis of the ellipse is perpendicular to that of tropism of particles. The result in accord with that of Lzumitanl and Hashimoto.[6]

Since the power spectrum image of 2DFT is corresponding to the SALS images,[4] the light-scattering theory, which is introduced in the following, can be

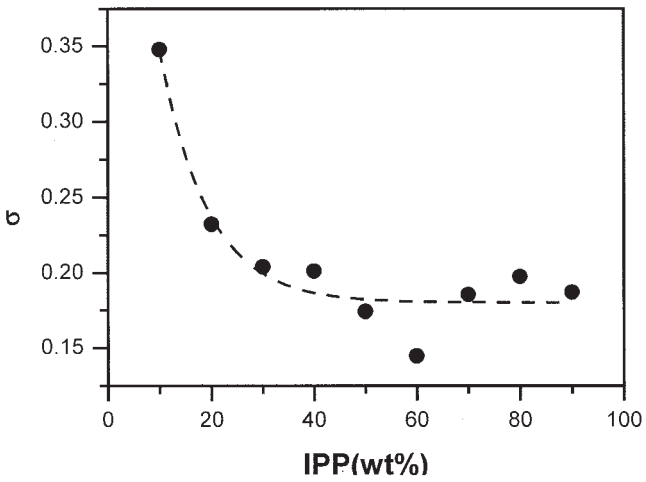

Figure 6 Variation of σ as a function of weight fraction of iPP in the blends of iPP/PcBR.

applied to study the structure and morphology of phases in the blends.

According to the results from Figure 7, we can find that the dispersed phase scatters in the matrix in the form of particles; therefore, the size of the particles can be computed using a correlation function. For this purpose, a modification of the Debye and Bueche and Khambatta et al.[7,8] description of scattering from random heterogeneous media is used to study the structure of blends, which gives for spherically symmetrical systems

$$I = 4\pi K V_s \eta^2 \int_0^\infty (r) \frac{\sin(hr)}{hr} r^2 dr \qquad (5)$$

where K is a proportionality constant and h = $(4\pi/\lambda)$ sin θ. $\overline{\eta^2}$ is the mean square fluctuation, η is the fluc-

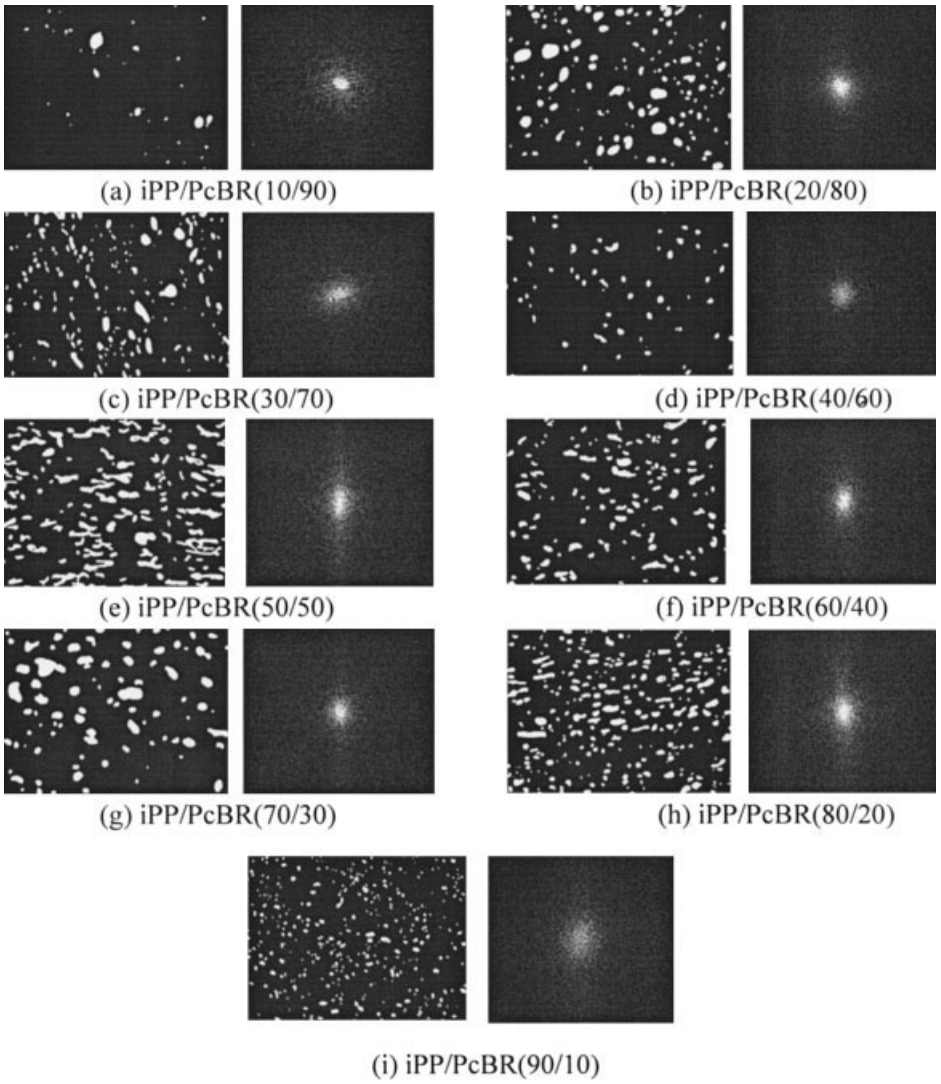

Figure 7 Binarized image in the left column and the corresponding 2DFT transformed patterns. (a) iPP/PcBR (10/90), (b) iPP/PcBR (20/80), (c) iPP/PcBR (30/70), (d) iPP/PcBR (40/60), (e) iPP/PcBR (50/50), (f) iPP/PcBR (60/40), (g) iPP/PcBR (70/30), (h) iPP/PcBR (80/20), (i) iPP/PcBR (90/10).

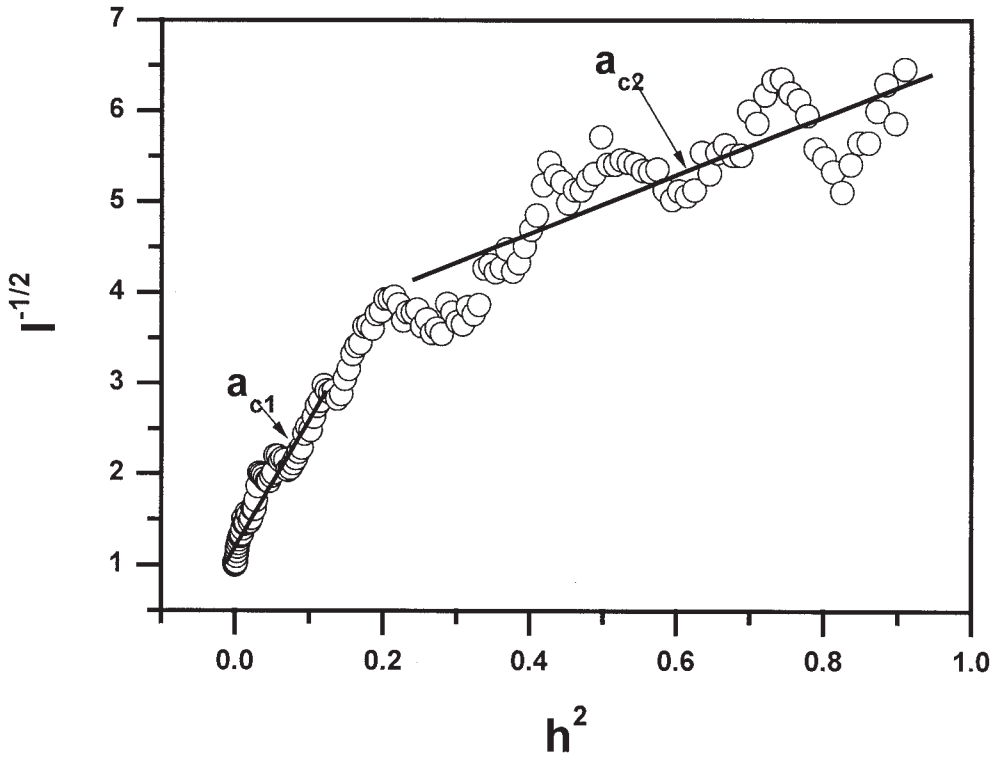

Figure 8 A plot of $I(h)^{-1/2}$ against h^2.

tuation in scattering power of the system, which for SALS is equal to the deviation $\alpha(r)$ in polarizability at a certain position from its mean value. r is the distance of different scattering units. $\gamma(r)$ represents the correlation function. For systems without a clearly defined structure, $\gamma(r)$ often decreases monotonically with r and can be described as

$$\gamma(r) = \exp(-r/a_c) \tag{6}$$

where a_c is defined as the correlation distance to describe the size of the heterogeneity. For dilute discrete particles, a_c is related to the particle size. For more concentrated systems, a_c depends upon both interparticle and intraparticle distances. It may be regarded as an average wavelength of the $\eta(r)$ fluctuations, whereas $\overline{\eta^2}$ is the mean-square fluctuation.

Substituting eq. (6) into eq. (5), one obtains

$$I(h) = K''\overline{\eta^2}a_c^3(1 + h^2a_c^2)^{-2} \tag{7}$$

Upon rearrangement, this gives

$$I(h)^{-1/2} = (K''\eta^2a_c^3)^{-1/2}(1 + h^2a_c^2) \tag{8}$$

Consequently, a plot of $I(h)^{-1/2}$ against h^2 should lead to a straight line having a ratio of slope to intercept of a_c^2. But a plot of $I(h)^{-1/2}$ against h^2 can lead to two straight lines (see Fig. 8), (for SALS where θ is small, the corresponding a_{c1} is due to scattering from large particles; and where θ leads to ∞, the corresponding a_{c2} is due to scattering from small particles). Indeed, there are marked peaks and troughs in the curve, especially when $h^2 > 0.2$, as in Figure 8, but this typical fluctuation will not affect our statistical results of a_{c2}. Similar methods were also used by Kawai.[9] Bauer and Pillai[10] depicted dimension of a_{c2} and a_{c1} parameters measured by the light scattering method and showed the physical significance of this function in Figure 9.

On the other hand, the volume of one scattering particle (v) is $4/3\pi a_{c2}^3$. If there are n such scatters in the correlation volume (V) and if c is the percentage of the dispersed phase (filler in the blends), then

$$V_c = nv \tag{9}$$

$$i.e., (a_{c2}/a_{c1})^3 = kc \tag{10}$$

An analysis may be made in terms of the approach of Debye and Bueche[7] for a random dispersion of two phases of volume fractions ϕ_1 and ϕ_2, and definite composition for which the ratio of interphase surface area S to the volume V is related to the correlation distance by

$$S/V = 4\phi_1\phi_2/a_c \tag{11}$$

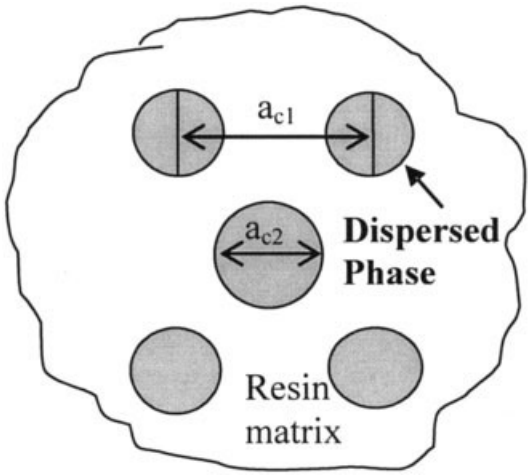

Figure 9 One-dimensional dispersed phase showing array a_{c1} and a_{c2} distance.

The average chord lengths $\bar{l}_1$ and $\bar{l}_2$ was defined in Figure 10, as discussed by Khambatta et al.[8] In Figure 10, $\bar{l}_1$ represents the mean length of the line segments through regions of phase 1. These chord lengths are given by

$$\bar{l}_1 = 4\phi_1/(S/V) \tag{12}$$

and

$$\bar{l}_2 = 4\phi_2/(S/V) \tag{13}$$

from which it follows that

$$\bar{l}_1 = a_c/\phi_2 \tag{14}$$

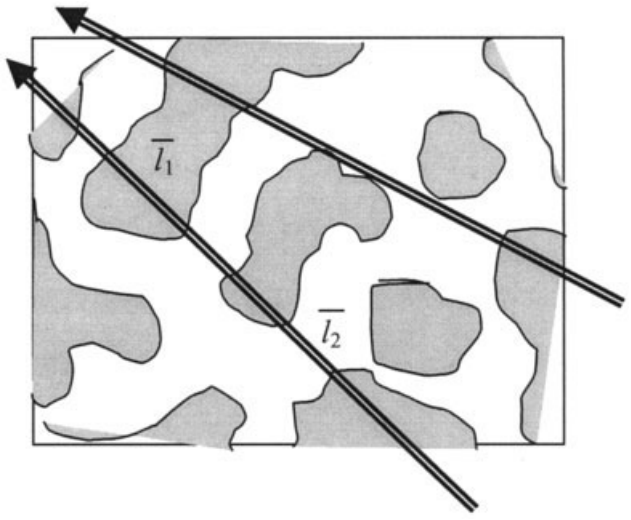

Figure 10 Chord lengths of a random two phases system. The average chord lengths are the average lengths of randomly drawn vectors passing through the two phases.

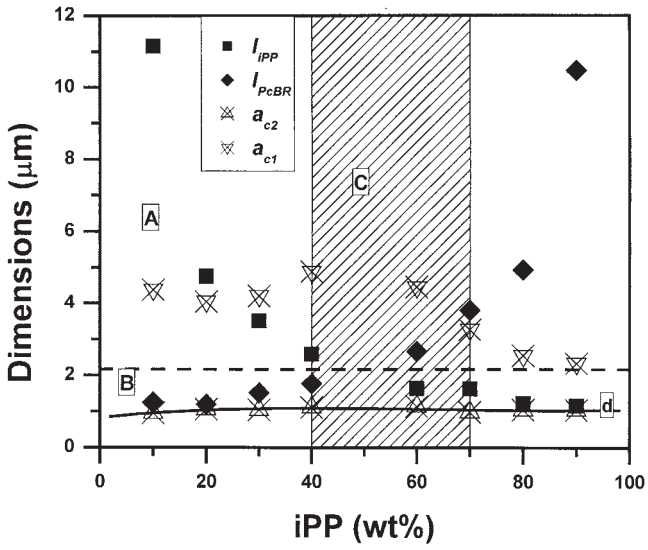

Figure 11 Relation of a_{c2} and average chord lengths with composition of the of iPP/PcBR blends.

and

$$\bar{l}_2 = a_c/\phi_1 \tag{15}$$

Here, average chord lengths can be calculated using a_{c2} by eqs. (14) and (15). The relation of $\bar{l}_{iPP}$ and $\bar{l}_{PcBR}$ with compositions of the blends of iPP/PcBR is shown in Figure 11.

The value of $\bar{l}_{PcBR}$ rises quickly with the iPP content increasing, while the value of the variation for $\bar{l}_{iPP}$ decreases rapidly. In region A, values of structure parameters describe sizes of continuous phases, and in region B, they express sizes of dispersed phases. Curve d shows dimension of dispersed phases in the blends, and the relation of a_{c2} with compositions of the blends is about the same. Comparing the relation of a_{c1} with compositions of the blends with continuous phases, though Inoue et al.[11] defines that a_{c1} shows large particles in the blends, the definition of Bauer and Pillai is more reasonable according to results of Figure 11. Region C is where phase inversion occurs, and the variation of value of a_{c2} and average chord lengths with compositions of the blends deviated from the law in this region. That is, before region C, iPP is dispersed phase, and PcBR is dispersed phase after C.

Additionally, The interphase surface area S in binary blends can be calculated using correlation distance a_c,[7,12] it follows that

$$S = 4\phi_1(1 - \phi_1)/a_c \tag{16}$$

Mean diameter (size) of disperse phases is defined by

$$D_S = \sum_n D_i^3 \Big/ \sum_n D_i^2 \tag{17}$$

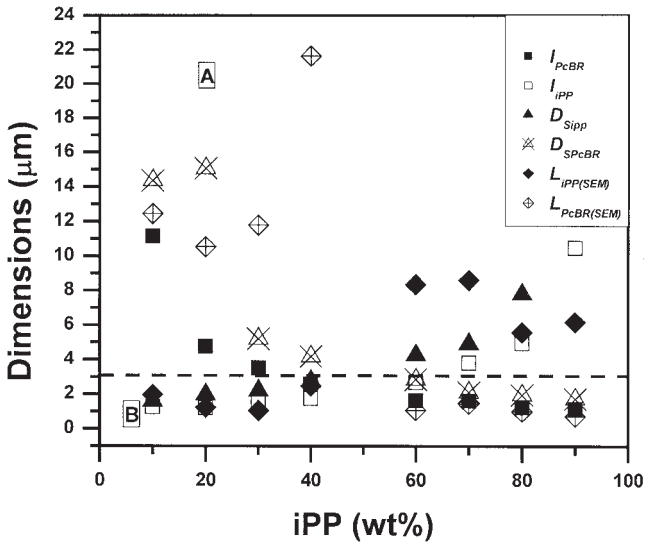

Figure 12 Relation of mean diameters and average chord lengths with composition of the of iPP/PcBR blends.

D_i is diameter of ith particle (dispersed phases). n is the amount of particles. The mean diameter can be calculated by SALS, which is given by

$$D_S = \sum_n D_i^3 \Big/ \sum_n D_i^2 = 6 \times \sum_n \frac{1}{6}\pi D_i^3 \Big/ \sum_n \pi D_i^2 = 6\phi_1/S \tag{18}$$

The mean diameter (D_S) is calculated using SALS. Figure 12 shows this result. The variation of mean diameters is the same as average chord length l. So, the mean diameter D_S is a valid parameter to describe the dimension of phases. In addition, we calculate the characteristic length L using SEM images. It can be found that the result of SEM is in accordance to that of SALS.

As mentioned above, the power spectrum of 2DFT is equivalent to images of SALS, thus, corresponding structure parameters can be obtained applying the light-scattering theory to the power spectrum of 2DFT.

The correlation distances have been calculated applying eqs. (14) and (15) to the power spectrum images (Table III and Fig. 13). Comparing Figure 13 with Figure 11 in variation rule of different parameters, it can be found that the change of $\bar{l}_{\text{fiPP}}$ and $\bar{l}_{\text{fPcBR}}$, a_{c1f} and a_{c2f} are the same as that of $\bar{l}_{\text{iPP}}$ and $\bar{l}_{\text{PcBR}}$, a_{c1} and a_{c2}.

The result indicates that 2DFT is an effective way to study the phase structure. Further more, we calculate the dimension of dispersed phases specially (see Fig. 4). Likewise, the result from the power spectrum is similar with that of SEM and SALS.

CONCLUSIONS

The structure parameters that can be used to characterize the structure and morphology of phases, such as correlation distances a_{c1} and a_{c2}, average chord lengths $\bar{l}_{\text{iPP}}$ and $\bar{l}_{\text{PcBR}}$, and mean diameter D_S have been calculated by data of SALS in the iPP/PcBR blends and their variation with compositions in the blends of iPP/PcBR is studied. The varied rule of structure parameters, especially structure parameters of dispersed phases, with compositions in the iPP/PcBR blends can be shown in the phase inversion region. This phase inversion region may be from 40 to 70 wt % iPP in the blends. Before 30 wt % iPP, the phase of iPP is the dispersed phase, and PcBR becomes the dispersed phase after 70 wt % iPP in the blends of iPP/PcBR.

TABLE III
Structural Parameter (a_c) of iPP/PcBR Alloys by SEM

iPP composition (wt %)	a_{c2} (μm)	a_{c1} (μm)
10	0.81	3.55
20	0.90	1.30
30	0.89	2.31
40	1.25	3.58
50	1.18	0.95
60	1.17	2.05
70	1.31	1.85
80	1.21	1.16
90	1.01	1.57

The structure and morphology of phases in the blends of iPP/PcBR have been examined by SEM, and binarized images of structure and morphology of phases have been obtained by graph-analysis technique. The sizes of dispersed phases, such as the mean diameter d_p of dispersed phases, characteristic lengths of two-phase, and the distribution of d_p in the blends of iPP/PcBR have been got from the binarized images. And the variation rule and dimension of d_p, L_{iPP}, and

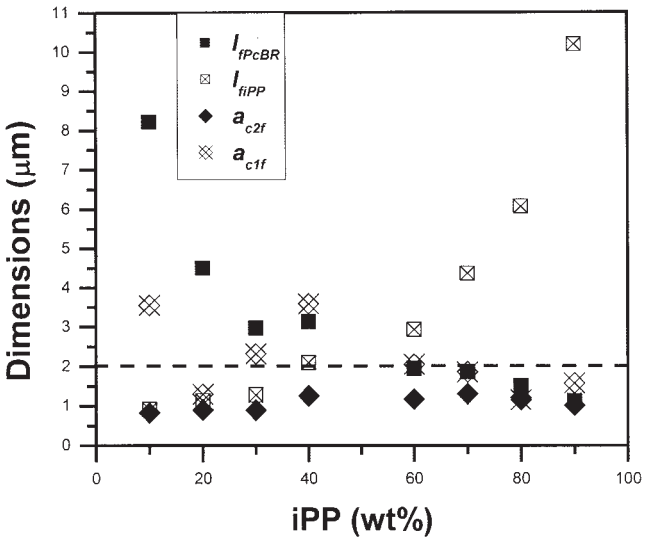

Figure 13 Relation of a_c and l with composition of the of IPP/PcBR blends on the power spetrum images of 2DFT.

L_{PcBR} are the same as that of structure parameters calculated by SALS. Within the region of compositions from 50 to 70 wt % iPP, the blends show a cocontinuous morphology, and the phase-inversion occurs in this region.

The distribution of sizes of dispersed phases in iPP/PcBR blends accords with the log-normal distribution and the distribution characterization of phases is relating to compositions in the blends of iPP/PcBR.

We obtained the power spectrum images that are equivalent to SALS images by 2DFT of binarized images. The correlation distances and average chord lengths have been calculated by intensity of the power spectrum images. These results, i.e., variation rule and dimension of structure parameters, are the same as results of SALS.

Comparing these results with that of SAXS in our second preceding paper,[2] we find that conclusions in this stufy are the same as results of SAXS. Obviously, SALS can only characterize micro-structure of iPP/PcBR system, but SAXS can study nano-structure of this system.

References

1. Sheng, J.; Qi, L.-Y.; Yuan, X.-B. J Appl Polym Sci 1997, 64, 2265.
2. Ma, G.-Q.; Yuan, X.-B.; Sheng, J.; Bian, D.-C. J Appl Polym Sci 2002, 83, 2088.
3. Paul, D. R.; Bucknall, C. B. Polymer Blends; Wiley-Interscience: New York, 2000.
4. Tanaka, H.; Hayashi, T.; Nishi, T. J Appl Phys 1986, 59, 3627.
5. Fang, K.-T.; Xu, J.-L. Statistics Distribution (Chinese); Science Press: Beijing, 1987.
6. Lzumitanl, T.; Hashimoto, T. J Chem Phys 1985, 83, 3694.
7. Debye, P.; Bueche, A. N. J Appl Phys 1949, 20, 518.
8. Khambatta, F. B.; Warner, F.; Russell, T.; Stein, R. S. J Polym Sci Polym Phys Ed 1976, 14, 1391.
9. Motegi, M.; Kawai, H. Fiber Ind 1970, 3, 86.
10. Bauer, R. G.; Pillai, P. S. In Toughness and Brittleness of Plastics; Deanin, R. D., Crugnola, A. M., Eds.; ACS Advances in Chemistry Series 154; American Chemical Society: Washington, DC, 1979; p 284.
11. Inoue, T.; Soen, T.; Motegi, M.; Kawai, H. Macromolecules 1970, 3, 87.
12. Moritani, M.; Inoue, T.; Motegi, M.; Kawai, H. Macromolecules 1970, 3, 433.